Chapter 14

H11: Hydrograph Routing

Contents

This problem was contributed by Peter E. Smith.

14.1 Problem Specification

H10 Hydrograph Routing

Focus routing evolution, numerical precision.

Channel bed slopes linearly downwards from upstream point F to downstream point L. The rectangular channel bed width B is 100 ft. At F, $x_F = 0$ ft, $Z_F = +150.00$ ft, such that

$$Z(x) = 150 - S_0 x \text{ [ft]} \tag{14.1.1}$$

where the bed slope S_0 is 0.001.

The upstream boundary conditions are

$$Q(x_F,t)\left[\frac{\text{ft}^3}{s}\right] = \begin{cases} 250 + \dfrac{750}{\pi}\left(1-\cos\dfrac{\pi t}{75}\right) & \text{for } 0 < t < 150\,[\text{minutes}] \\ 250 & \text{for } t \geq 150\,[\text{minutes}] \end{cases} \tag{14.1.2}$$

At L, x_L = 150,000 ft, $Z_L = +0.00$ ft and

$$\eta(x_L,t) = +1.7\ [\text{ft}] \text{ for all } t \tag{14.1.3}$$

Channel friction factor is constant at Manning $n = 0.045$.

Initial conditions at $t = 0$ are

$$\begin{aligned} \eta(x,0) &= Z(x) + 1.7\ [\text{ft}], \text{ i.e. constant flow depth} \\ Q(x,0) &= 250\ [\text{ft}^3/\text{s}] \end{aligned} \tag{14.1.4}$$

Compute and write to file in the STANDARD FORMAT the initial conditions at $t = 0$ and the model predictions for every time step to $t = 500$ minutes.

Use the fixed computational space step Δx ft and the fixed computational time step Δt s specified in the separate lines of Table 14.1 to define three separate problems - a, b and c.

Problem	Δx ft	Δt s
H11a	1000	60
H11b	2000	120
H11c	5000	300

Table 14.1: Space and Time Steps for Hydrograph Evolution

Report parts a, b and c as SEPARATE files.

14.2 Background

The expected response here is classical channel hydrograph routing. Initial conditions are uniform flow[1]; the normal depth is $h_n = 1.7$ ft. The flood hydrograph enters through the upstream boundary as a $Q(t)$ trace. The computations are terminated before the downstream boundary can have any influence. The initial Courant Number for all three parts is $\mathbf{Cr} = (gh_n)^{1/2}\Delta t/\Delta x = 0.44$, well within the expected capabilities of any viable numerical code.

The specific foci of these problems are

[1]For a flow of 250 ft^3/s, the normal depth is actually 1.7085 ft, and the critical depth 0.58 ft. With the Equation 14.1.3 downstream control, the steady-state gradually varied flow profile is an M_2 profile extending upstream from $h = 1.7$ ft at x_L to the normal depth of 1.7085 ft. This is a gradual but very small increase in depth in the upstream direction.

But the Equation 14.1.4 initial conditions are not exactly at steady state. There is an immediate transient reaction from x_L, that initiates the eventual evolution to the steady-state M_2 profile. But these adjustments are quite small, and generally not observable in the subsequent surface plots.

- spatial resolution of the response
- Q-boundary forcing
- routing of a hydrograph

14.3 Contra Costa Water District

The CCW model apparently could not provide solutions for any of problems H11a through H11c. A predicted solution for a re-defined problem with $\Delta x = 25$ ft and $\Delta t = 1$ s was presented, at which the Courant Number is 0.30.

The CCW-predicted solution field evolution is shown in Figure 14.1. Both the η and Q evolution[2] show the expected hydrograph routing. The hydrograph peak is attenuated with propagation distance, the width of the hydrograph increases, with the trailing face becoming much more gradual than the leading face. This is the expected response.

Just why the CCW model could provide a solution for Courant Number 0.30 but not 0.44 is a cause for concern. In a response[3], CCW have cited the Courant-Friedrichs-Lewy (CFL) stability criterion, that requires that the new time step be within the characteristic cone of influence:

$$\mathbf{CFL} = \frac{\left[Q/A \pm \sqrt{gA/b}\right] \Delta t}{\Delta x} \leq 1 \tag{14.3.1}$$

The **CFL** criterion with the plus sign is CCW's definition of Courant Number in the table reproduced in the footnote. This **CFL** criterion is certainly a legitimate requirement for the CCW three-point method characteristics algorithm, but the footnote table together with Figure 14.1 suggest an upper bound of about 0.75 for this problem. This is well within the **CFL** criterion. Numerical instability is not expected.

[2]The stepped response in the trailing edge of the η evolution is not a concern. It is a direct consequence of strict adherence to the 4 significant figures in the STANDARD FORMAT data files.

[3]The following commentary was provided by CCW (Shum, 27 April 2001): "The problems ... are caused by large discretization errors at the large grid sizes prescribed and not primarily because of stability (Courant number) consideration.

The problem is for a channel with water at an initial depth of 1.7 feet and an inflow that increases to a maximum of $Q_{\max} = 250 + 1500/\pi \approx 727$ cfs at $t = 75$ minutes. Estimates of the Courant number, accounting for both the shallow water celerity and flow velocity, show the following variation with water depth at $Q_{\max}$:

Water Depth (ft)	Flow Velocity (ft/sec)	Shallow Water Wave Celerity (ft/sec)	Flow + Celerity (ft/sec)	Courant Number
2.0	3.64	8.02	11.7	0.70
3.0	2.42	9.83	12.3	0.74
4.0	1.82	11.35	13.2	0.79

As truncation errors increase with grid size, numerical simulation breaks down as the Courant Number in these simulations are close to the von Neumann criterion (threshold) of 1.0. ... the computational breakdowns can be easily explained by the fact that the FDM uses an explicit scheme, and large truncation errors when the grid size is large lead to numerical instability at large Courant Numbers."

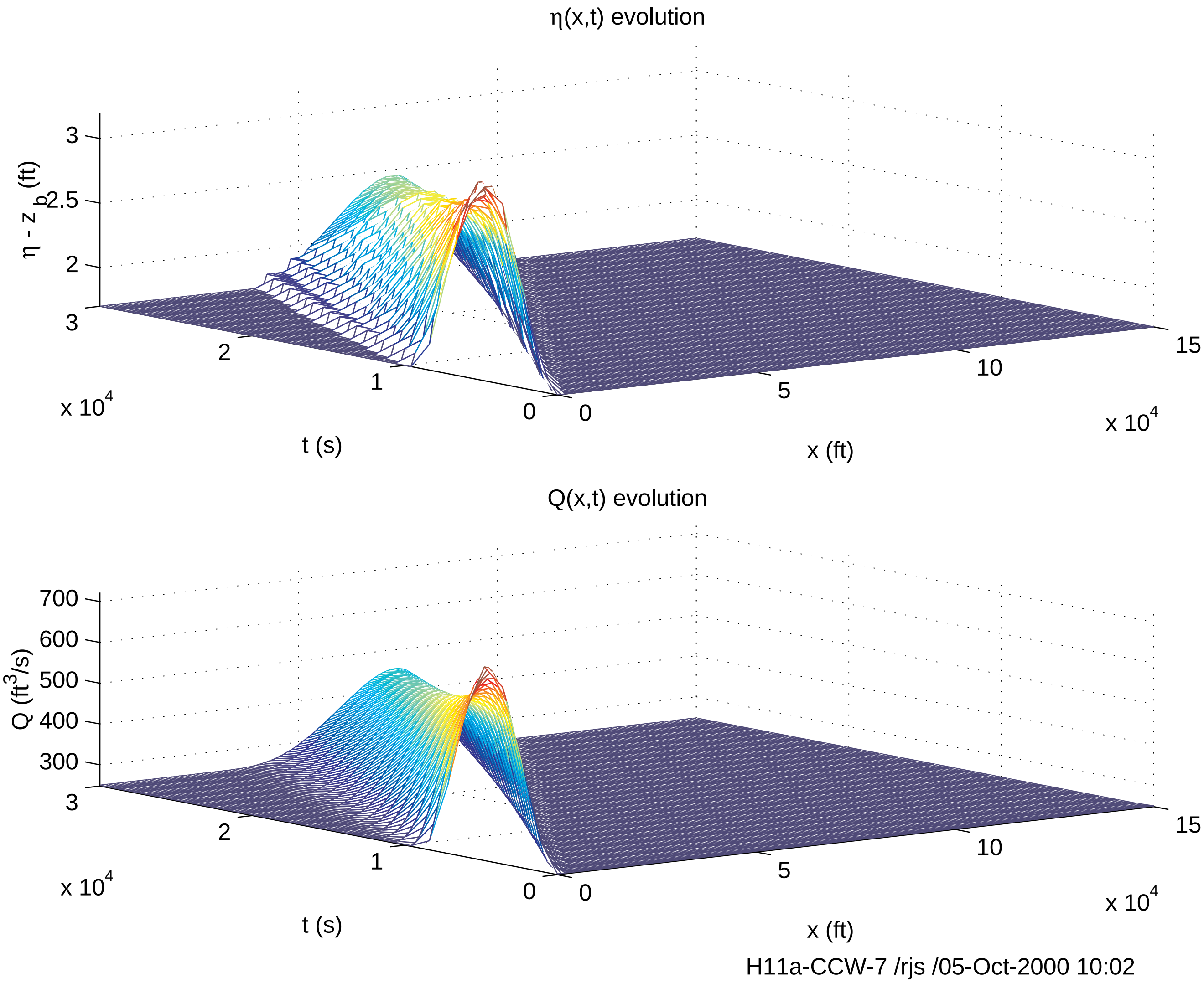

Figure 14.1: Modified H11 CCW-predicted solution field evolution.

It is more likely that the difficulty is a consequence of implicit numerical diffusion (Hoffman 1992, pages 727-8). The truncation error is O(Δt, Δx^2, $\Delta x^2/\Delta t$). Numerical diffusion is proportional to $\Delta x^2/\Delta t$, which is 16,667 for H11a, 33,333 for H11b and 83,333 for H11c, but only 625 for the $\Delta x = 25$ ft and $\Delta t = 1$ s problem in Figure 14.1. The parameters of the H11 problem seem to have stretched the CCW three-point method characteristics algorithm well beyond its range of applicability.

This difficulty with the CCW algorithm can be controlled, as the potential impact of numerical diffusion can be anticipated. These limits of applicability are rather fundamental and need to be recognized.

14.4 Department of Water Resources

The DWR-predicted[4] solution field evolution for problem H11a is shown in Figure 14.2. Both the η and Q evolution show the expected hydrograph routing. The hydrograph peak is attenuated with propagation distance, the width of the hydrograph increases, with the trailing face becoming much more gradual than the leading face. This is the expected response.

The equivalent results for problems H11b[5] and H11c[6] are shown in Figures 14.3 and 14.4. The H11b result, at Δx = 2,000 ft, is visually identical to the H11a result. The much coarser resolution, Δx = 5,000 ft, of the H11c problem has a significant impact on the response pattern at the steeper leading edge. The short-wavelength oscillations here are the tell-tale signs of a resolution-challenged response. Nevertheless, this is the expected response.

[4] The DWR data file reports the computational time step Δt as 1 s; it was apparently the required 60 s. The time step has been changed to 60 s for the following analyses.

[5] The DWR data file reports the computational time step Δt as 1 s; it was apparently the required 120 s. The time step has been changed to 120 s for the following analyses.

[6] The DWR data file reports the computational time step Δt as 1 s; it was apparently the required 300 s. The time step has been changed to 300 s for the following analyses.

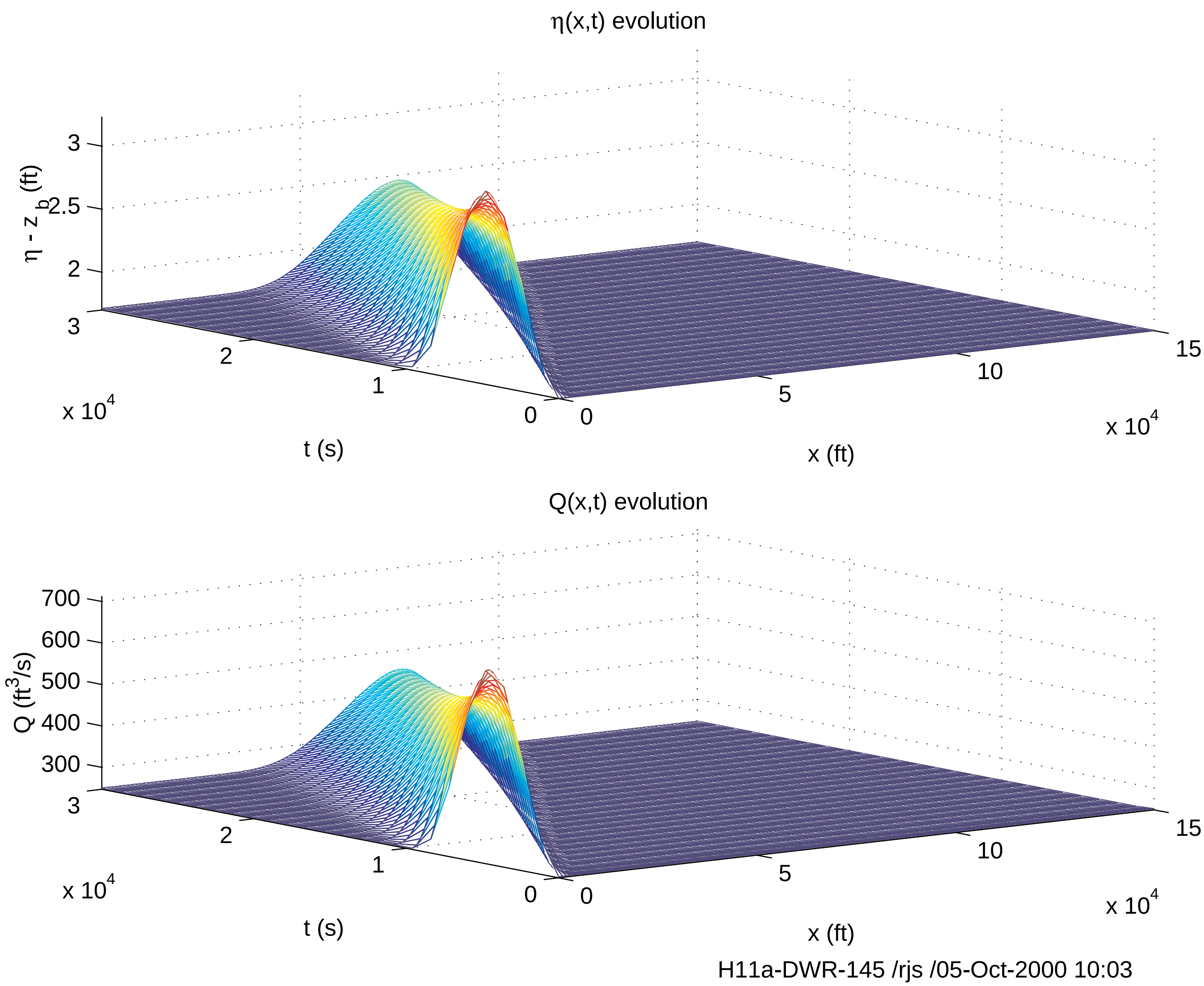

Figure 14.2: H11a DWR-predicted solution field evolution.

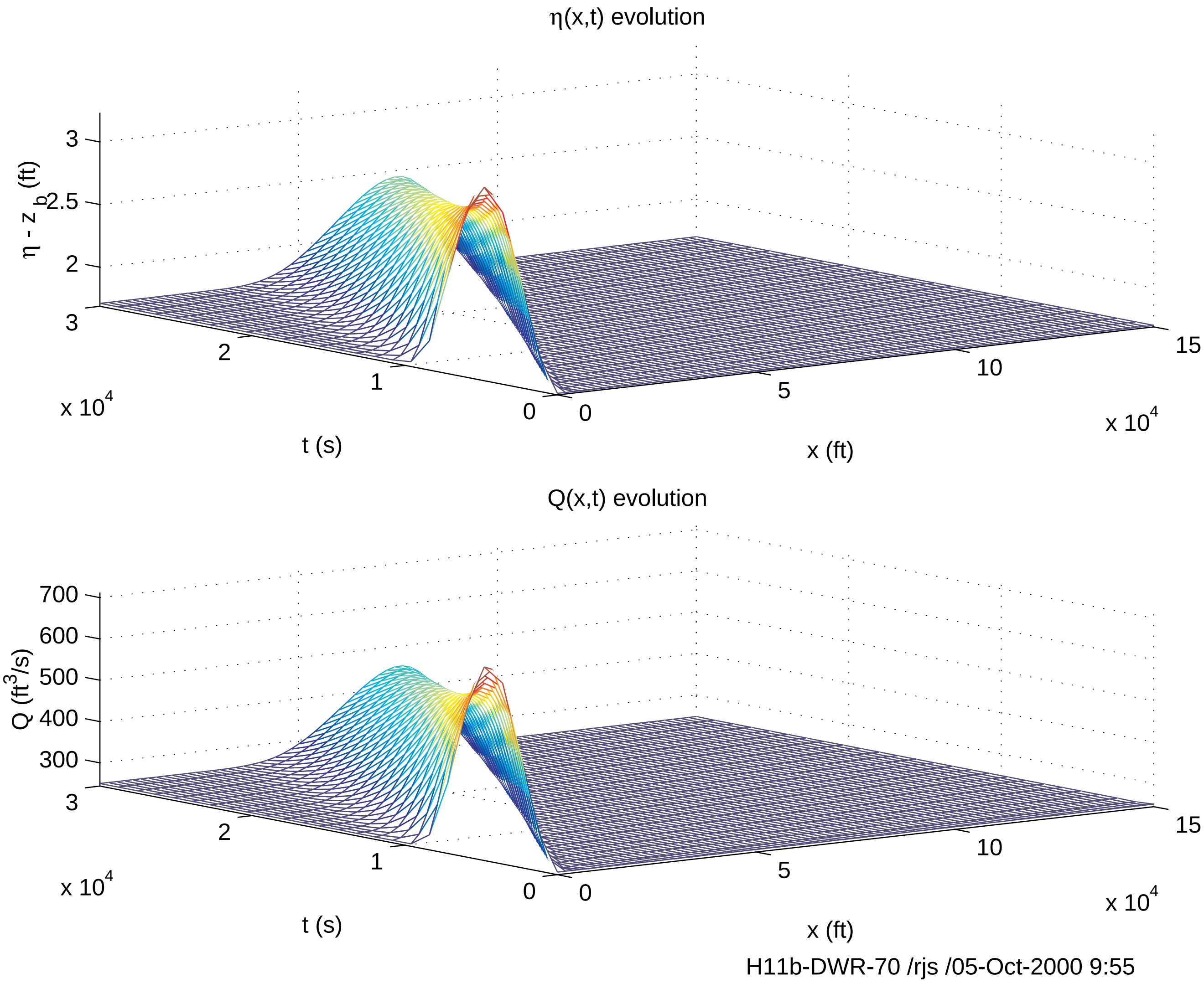

Figure 14.3: H11b DWR-predicted solution field evolution.

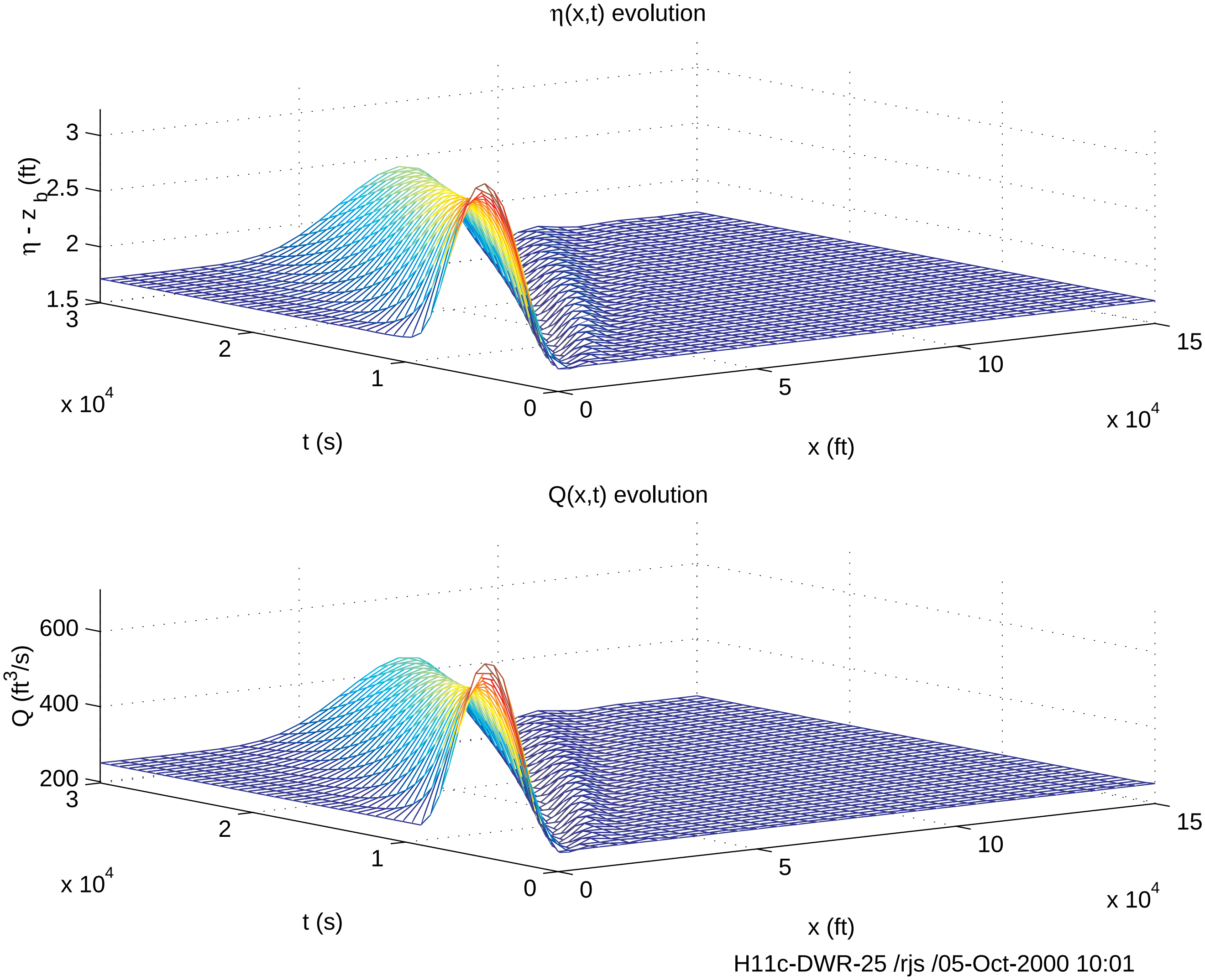

Figure 14.4: H11c DWR-predicted solution field evolution.

14.5 Resource Management Associates

The RMA-predicted[7] solution field evolution for problem H11a is shown in Figure 14.5. Both the η and Q evolution show the expected hydrograph routing. The hydrograph peak is attenuated with propagation distance, the width of the hydrograph increases, with the trailing face becoming much more gradual than the leading face. This is the expected response.

The equivalent results for problems H11b and H11c are shown in Figures 14.6 and 14.7. The H11b result, at Δx = 2,000 ft, is visually identical to the H11a result. The H11c prediction, at the much coarser resolution, Δx = 5,000 ft, has hints of short-wavelength oscillations that are the tell-tale signs of a resolution-challenged response. Given the very coarse resolution, this is almost a satisfactory result. Overall, this is the expected response.

[7]RMA changed the both the Equation 14.1.3 boundary condition and the Equation 14.1.4a initial conditions from 1.7 ft to 1.7114 ft, presumably to avoid the small transient from x_L. 1.7114 ft is the RMA model estimate for normal depth at a flow of 250 ft^3/s, corresponding to a units correction factor of 1.486 in the Manning formula. Equation 2.4.3c has 1.49, which corresponds to a normal depth of 1.7085 ft. These differences are not significant, but they do show up in subsequent figures, Figures 14.13 through 14.15.

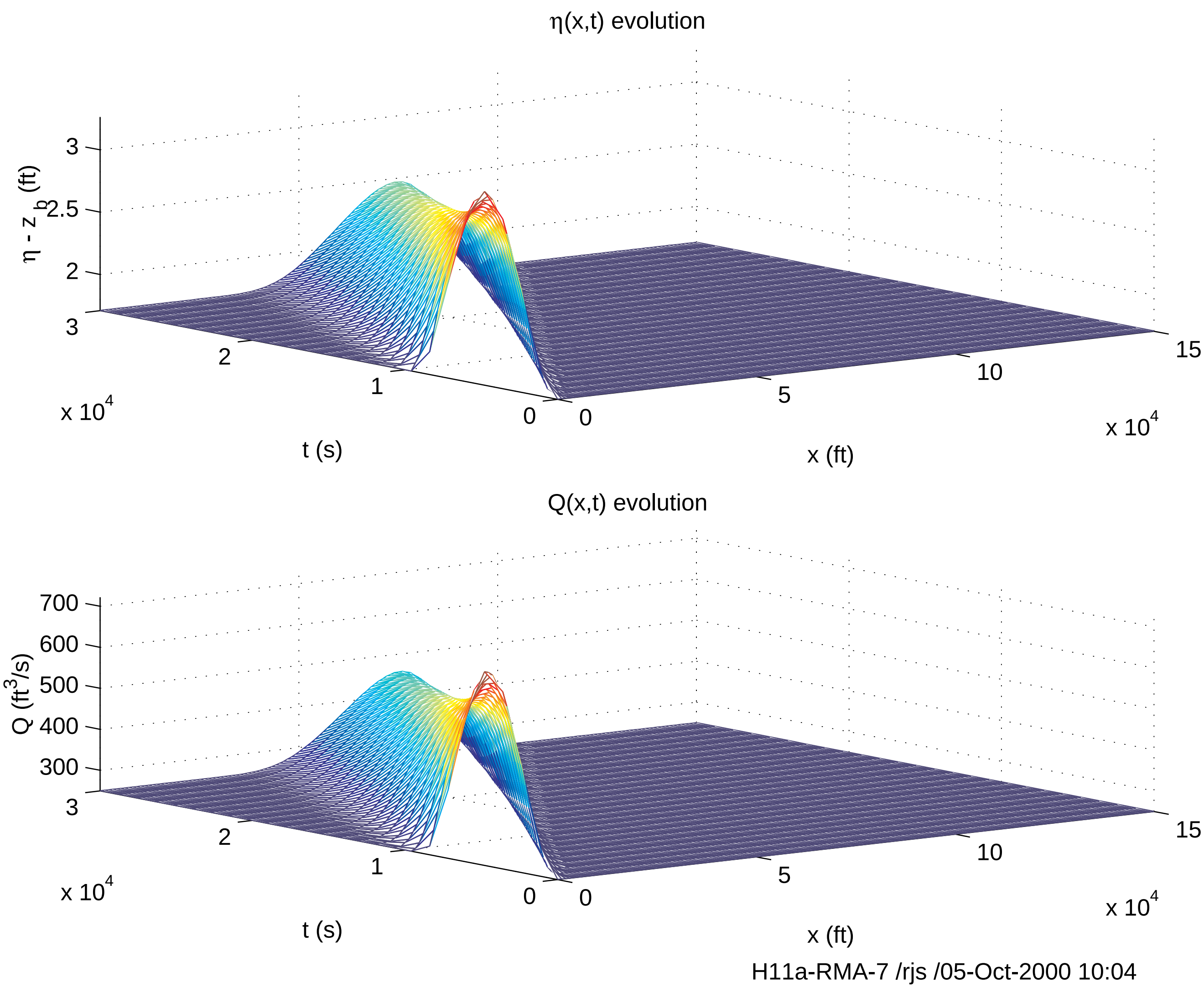

Figure 14.5: H11a RMA-predicted solution field evolution.

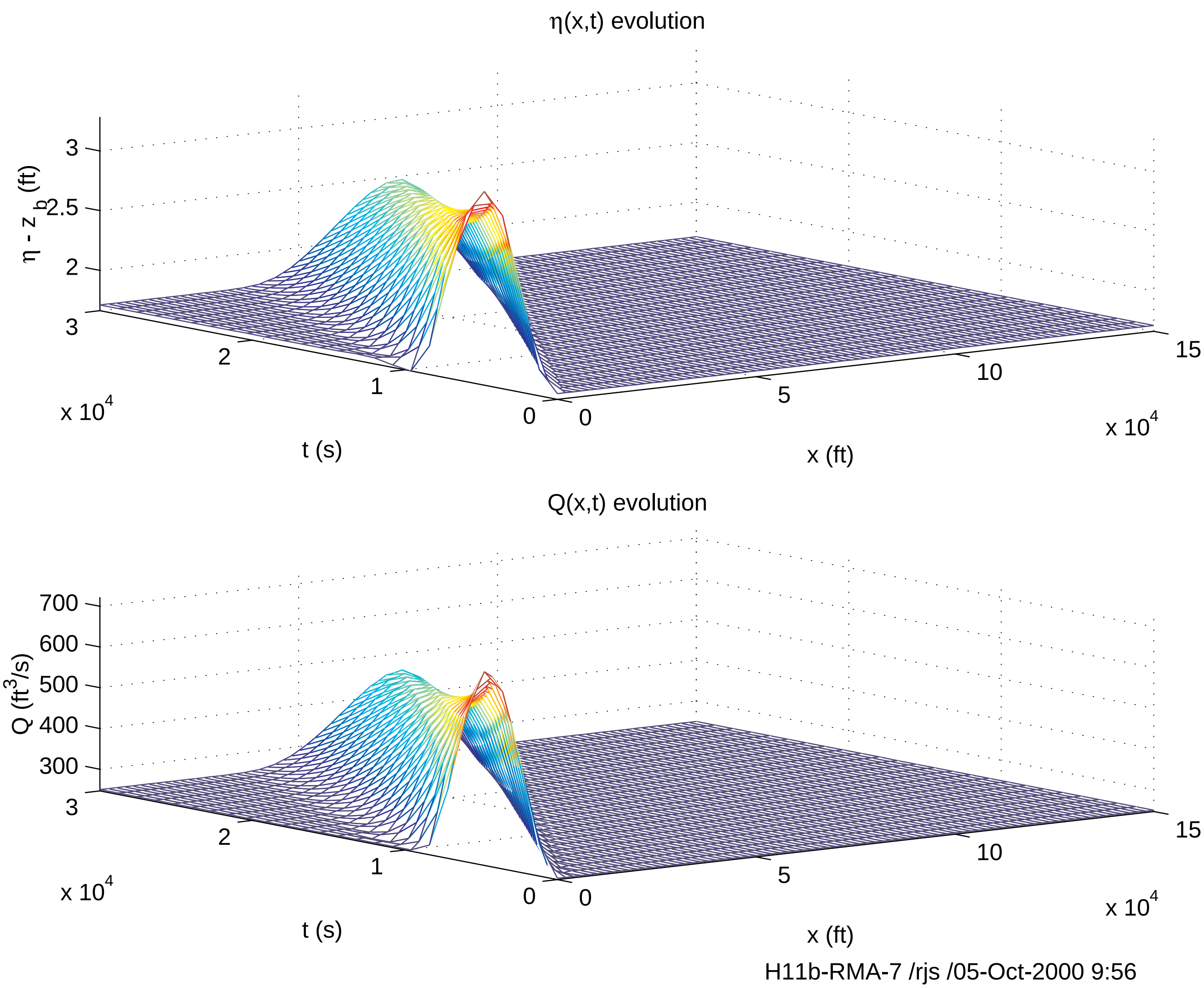

Figure 14.6: H11b RMA-predicted solution field evolution.

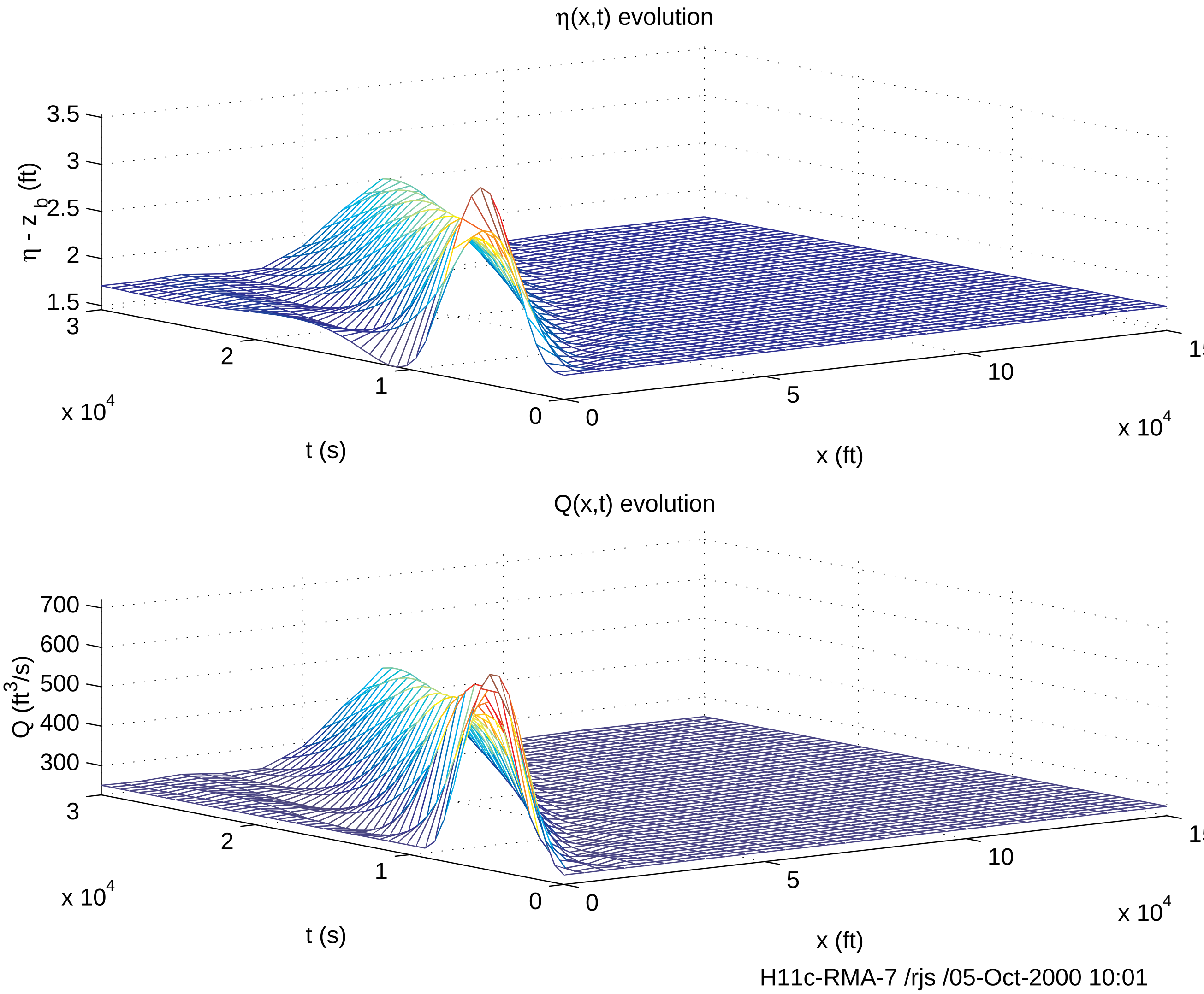

Figure 14.7: H11c RMA-predicted solution field evolution.

14.6 Response Comparisons

The primary objective of this series of problems is an evaluation of the spatial resolution of the participant numerical codes. It would be convenient to compare each of these results to the correct result, and to focus a discussion of spatial resolution on the differences from the correct result.

But what is the correct result? Each of the above results is a model approximation. None are exact. An analytical solution is not possible. A reasonable datum for comparison is another credible model, not at the same spatial resolution but at a much smaller spatial resolution than H11a. The adopted datum is ESTFLOW model predictions for $\Delta x = 250$ ft, with predictions in adaptive time-step mode[8]. The predictions, η_{Datum} and Q_{Datum}, are visually identical to Figures 14.2(DWR) and 14.5(RMA).

As an illustration of what might be expected, Figure 14.8 shows the difference prediction, respectively $\eta - \eta_{\text{Datum}}$ and $Q - Q_{\text{Datum}}$, for H11a from the ESTFLOW code. The stem-and-marker symbols mark the path of the hydrograph peak in the datum solution. Even for the same numerical code, there is a clear impact of spatial resolution. The classical response is short wavelength oscillations in the neighborhood of the most rapidly-varied solution response, i.e. at the hydrograph peak. The location of an error trough immediately ahead the datum peak suggests an overall phase lag in the timing of the predicted peak.

[8]In adaptive time-step mode, the computational time step is locally and continuously adjusted to maintain a global error tolerance.

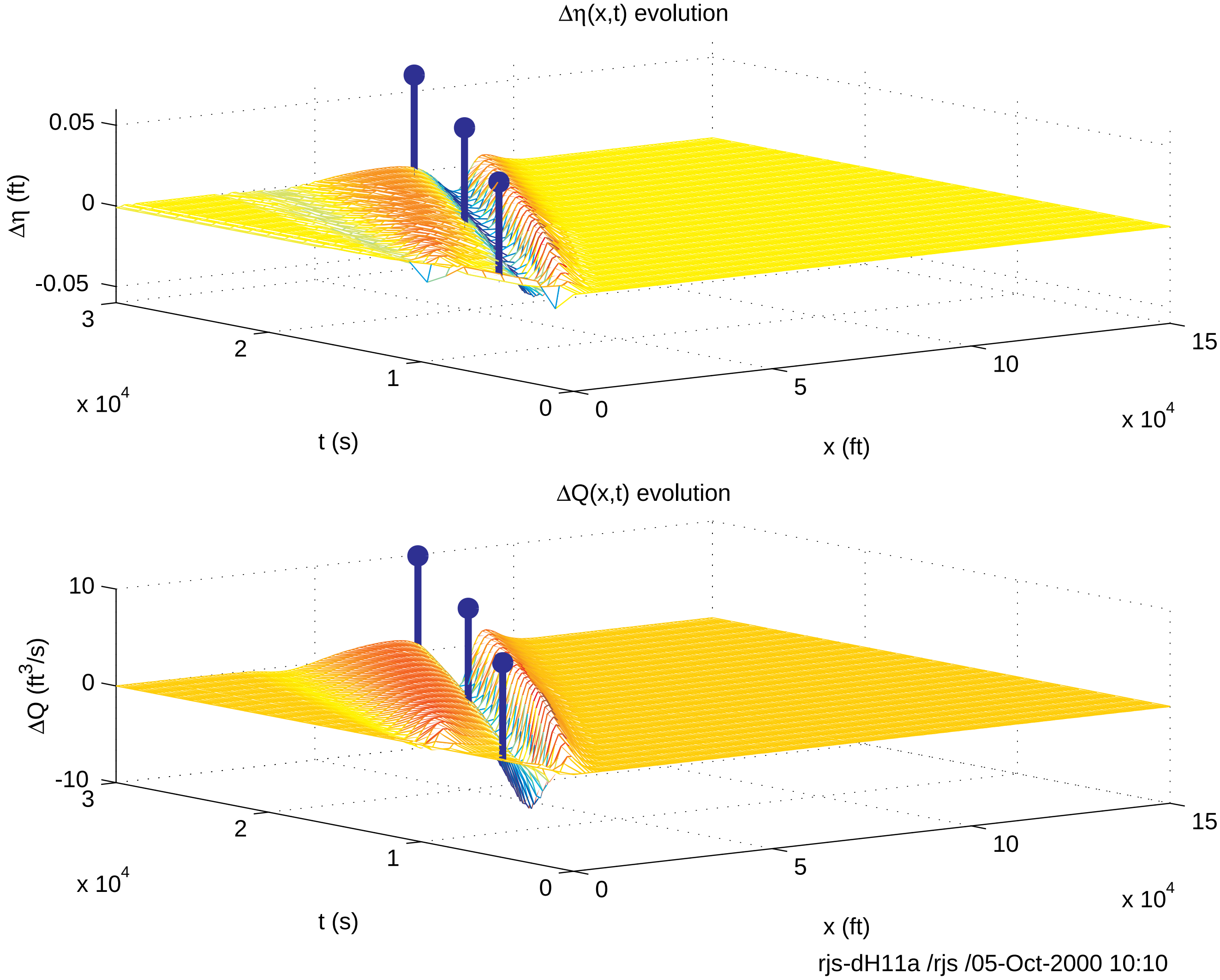

Figure 14.8: Error evolution in H11a ESTFLOW prediction.

14.6.1 Contra Costa Water District

Figure 14.9 is the difference prediction for H11 from the CCW code. Recall here that spatial resolution was $\Delta x = 25$ ft and the computational time step was $\Delta t = 1$ s. Interpretation of the $\Delta\eta$ evolution is confused by the data file truncation identified above, but the ΔQ has no such difficulty. The deep error trough immediately ahead the datum peak suggests an overall phase lag in the timing of the predicted peak. But the CCW prediction adopted a much finer resolution than the datum solution ($\Delta x = 25$ ft compared to $\Delta x = 250$ ft), and any interpretation is not secure!

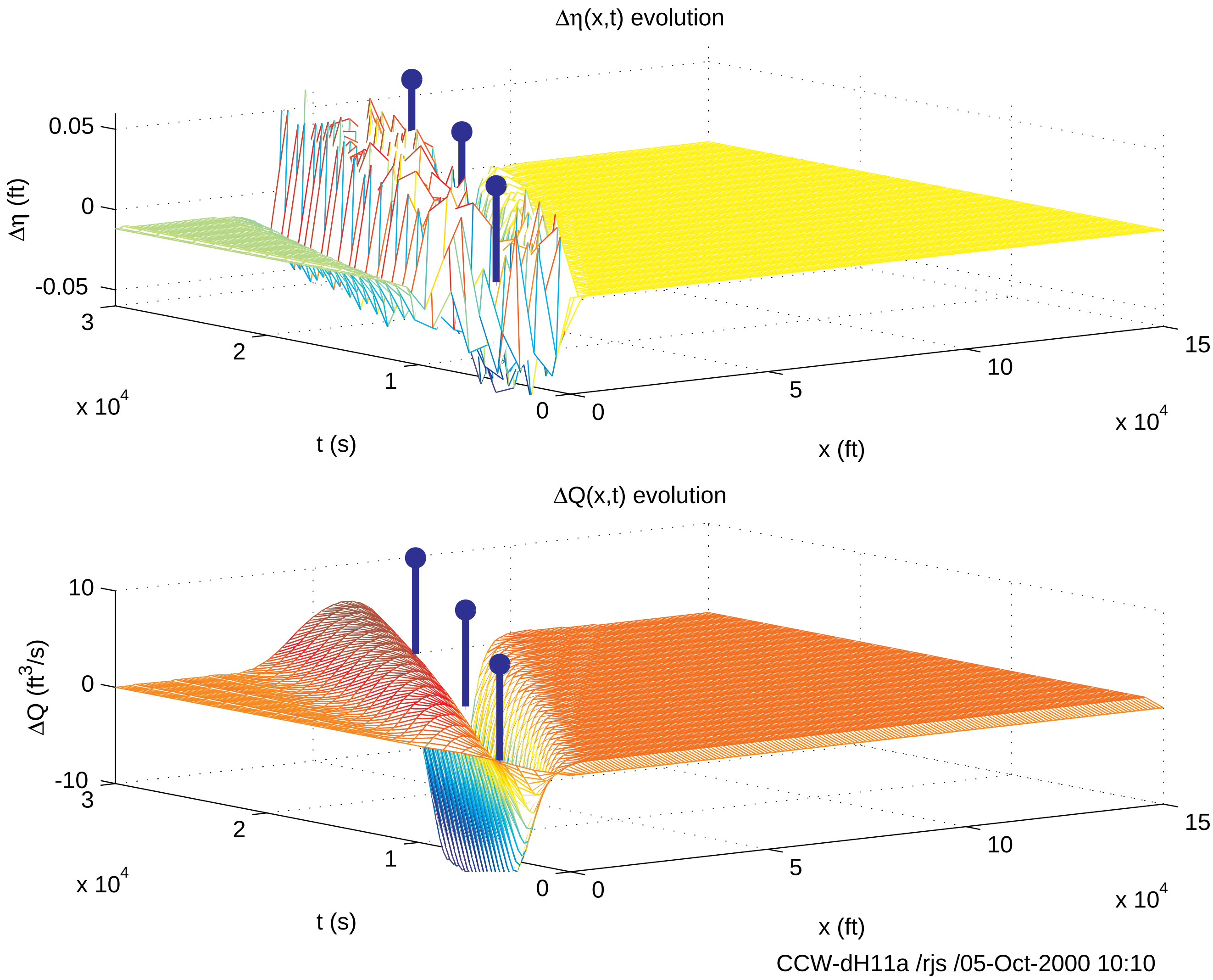

Figure 14.9: Error evolution in H11 CCW prediction.

14.6.2 Department of Water Resources

Figures 14.10 through 14.12 are the difference prediction for H11 from the DWR code. For H11a, the error ridge immediately ahead the datum peak suggests an overall phase lead in the timing of the predicted peak. The initial transients evident in Figure 14.10 (but not in Figure 14.8) suggest that the DWR model has some difficultly with upstream Q boundary conditions. For H11b, a similar but amplified trend is seen. This trend continues to H11c. The increasing spatial resolution seems to low-pass filter the the initial transients. The observed decline in precision with increasingly poorer spatial resolution is the expected response.

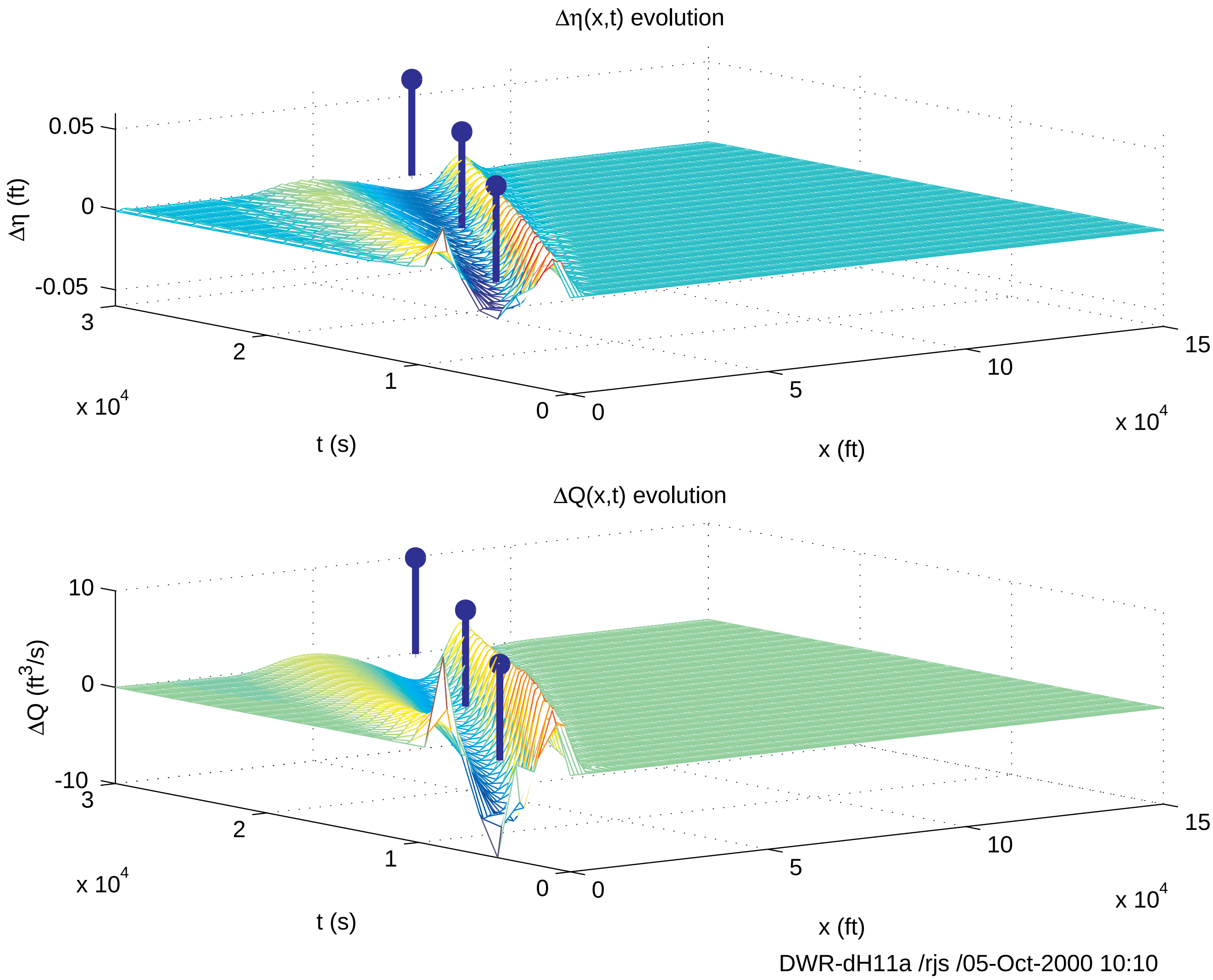

Figure 14.10: Error evolution in H11a DWR prediction.

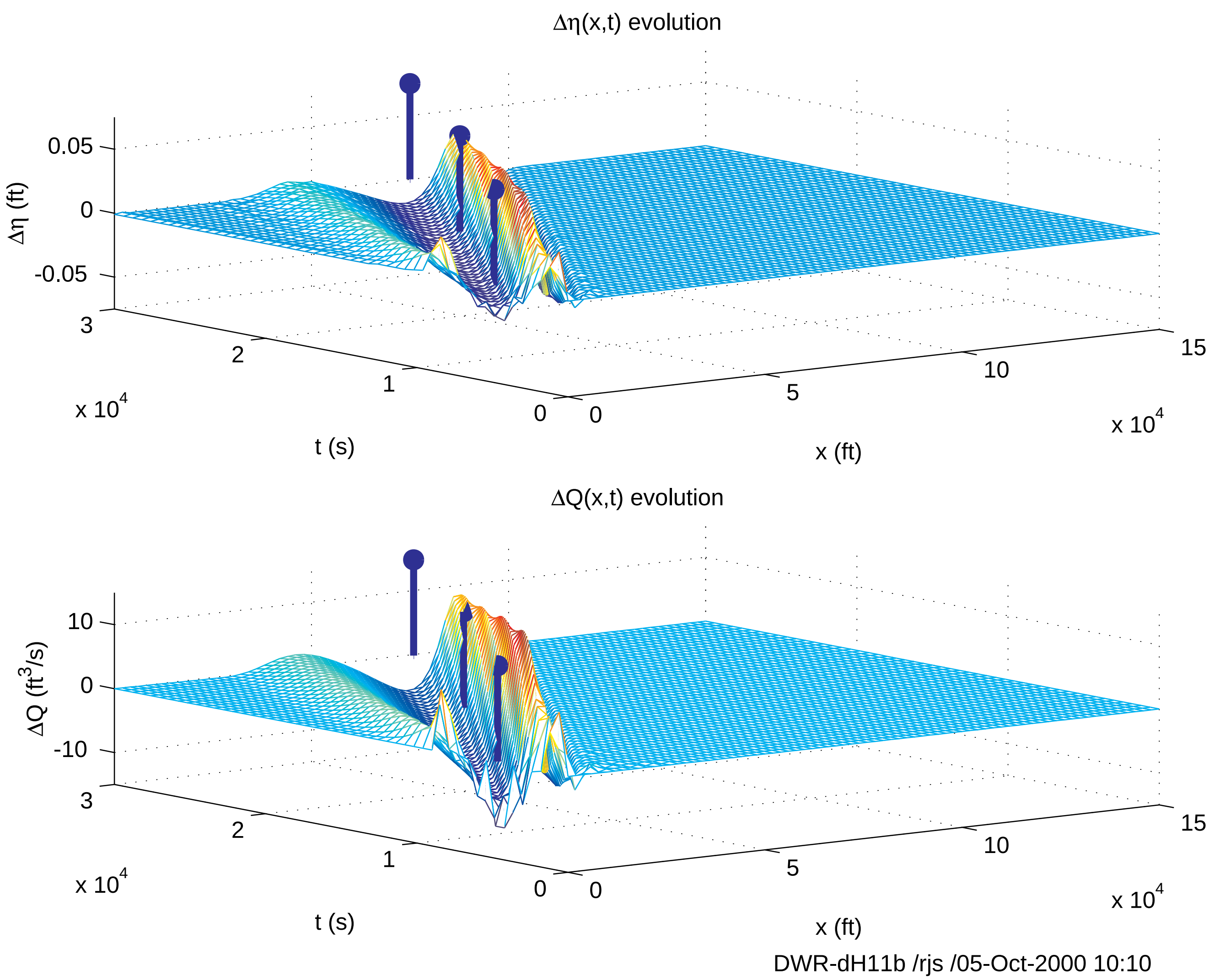

Figure 14.11: Error evolution in H11b DWR prediction.

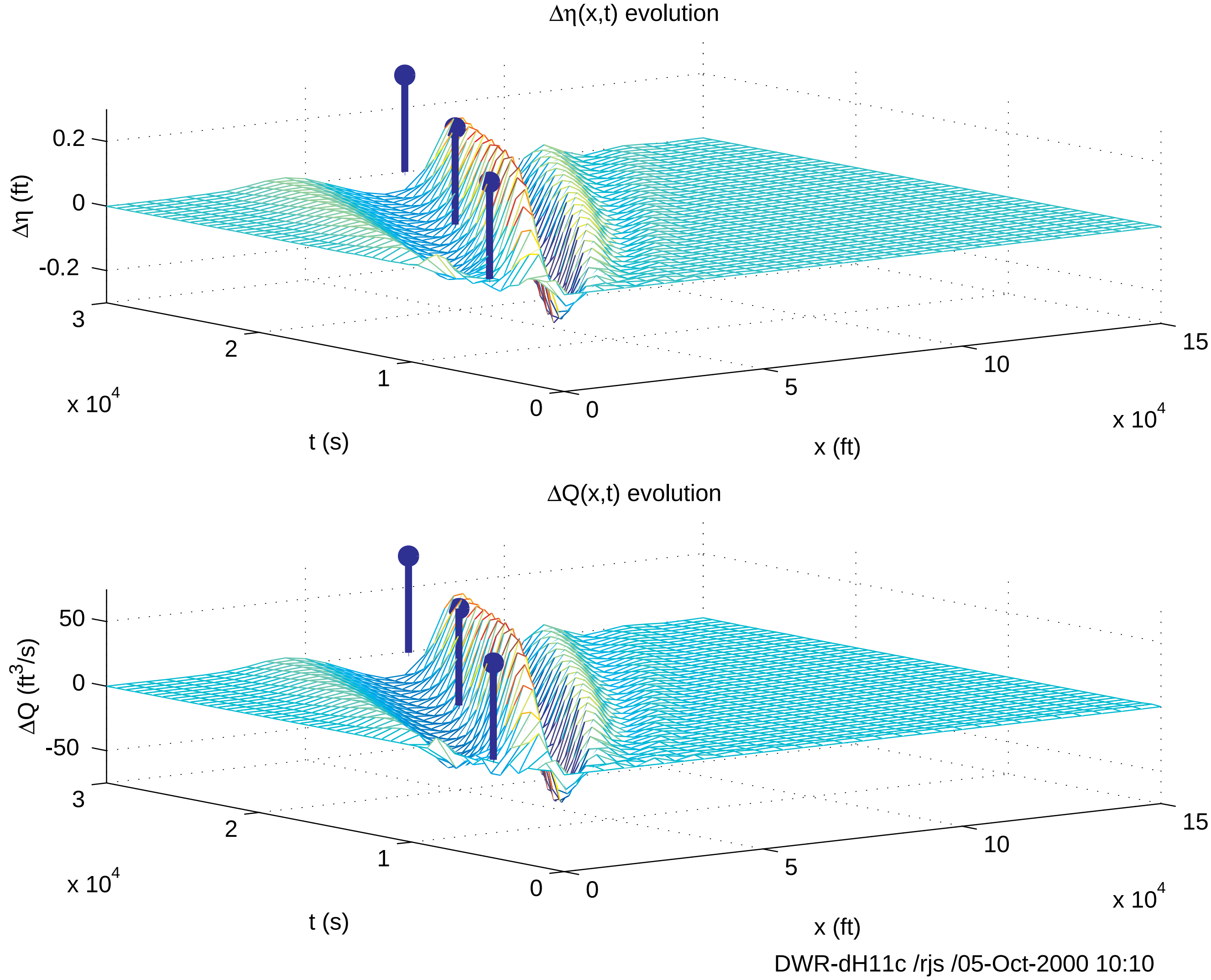

Figure 14.12: Error evolution in H11c DWR prediction.

14.6.3 Resources Management Associates

Figures 14.13 through 14.15 are the difference prediction for H11 from the RMA code. For H11a, the error ridge immediately ahead the datum peak suggests an overall phase lead in the timing of the predicted peak. The initial transients evident in Figure 14.13 (but not in Figure 14.8) suggest that the RMA model has some minor difficultly with upstream Q boundary conditions, though not as severe as the DWR model (Figure 14.10).

A notable feature of the H11a prediction is a global downstream influence. There appears to be a sharp step in both $\Delta\eta$ and ΔQ downstream of the hydrograph, where there should be no such influence. But RMA have changed[9] both the initial conditions and the downstream boundary condition. There is accordingly a step change from the datum solution, which is precisely what is observed. This response is expected, and does not suggest a problem.

For H11b, a similar but amplified trend is seen. For H11c, the amplification continues but there is now an error trough immediately ahead the datum peak suggests an overall phase lag in the timing of the predicted peak. The observed decline in precision with increasingly poorer spatial resolution is the expected response. Error magnitudes are generally smaller than the corresponding DWR solutions.

14.6.4 Summary

Overall, the H11a errors are small and follow the expected pattern. H11b and H11c errors are increasingly larger, but also follow the expected pattern.

REFERENCES

Hoffman, J. D. (1992). *Numerical Methods for Engineers and Scientists*. McGraw-Hill, New York.

[9]See §14.5

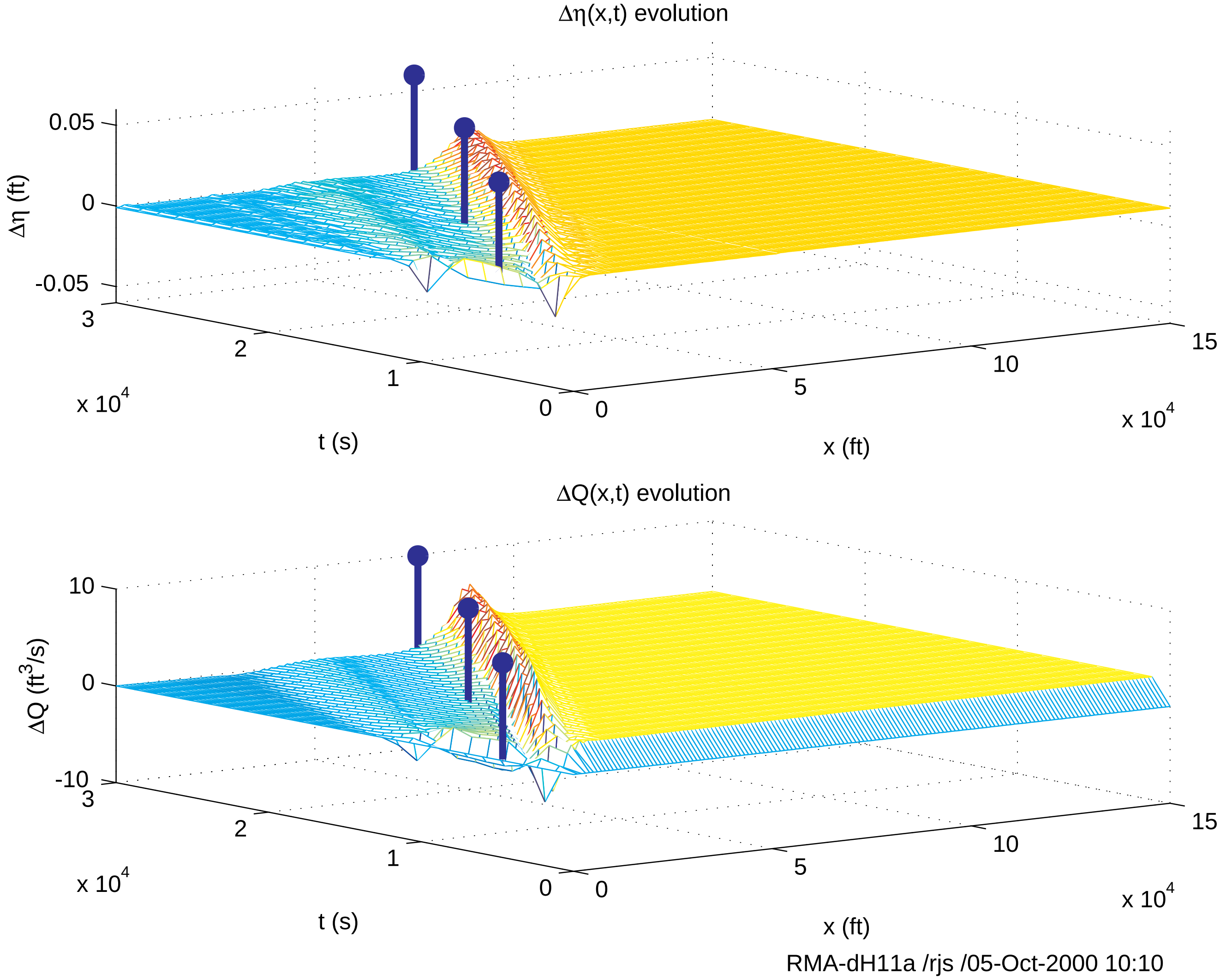

Figure 14.13: Error evolution in H11a RMA prediction.

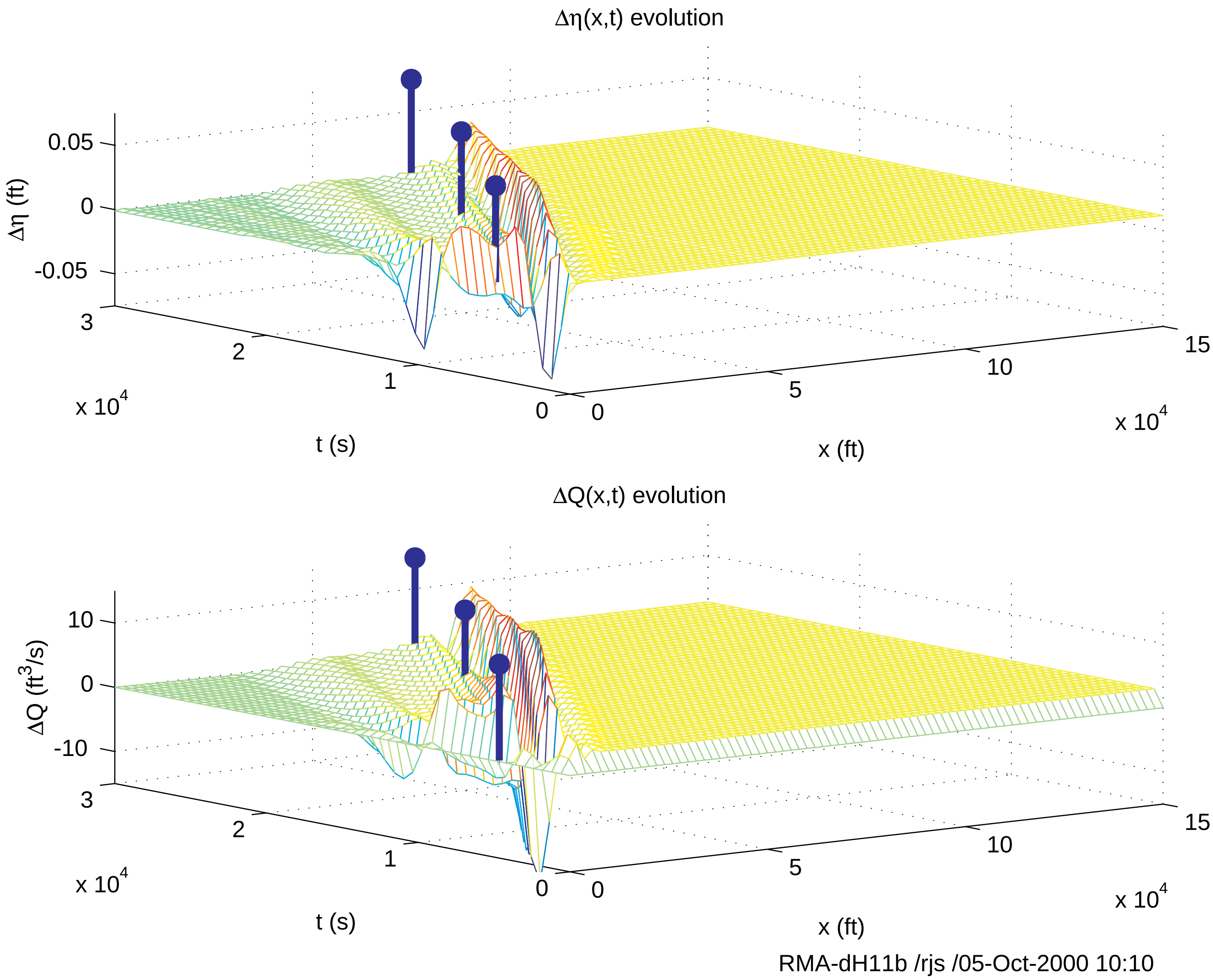

Figure 14.14: Error evolution in H11b RMA prediction.

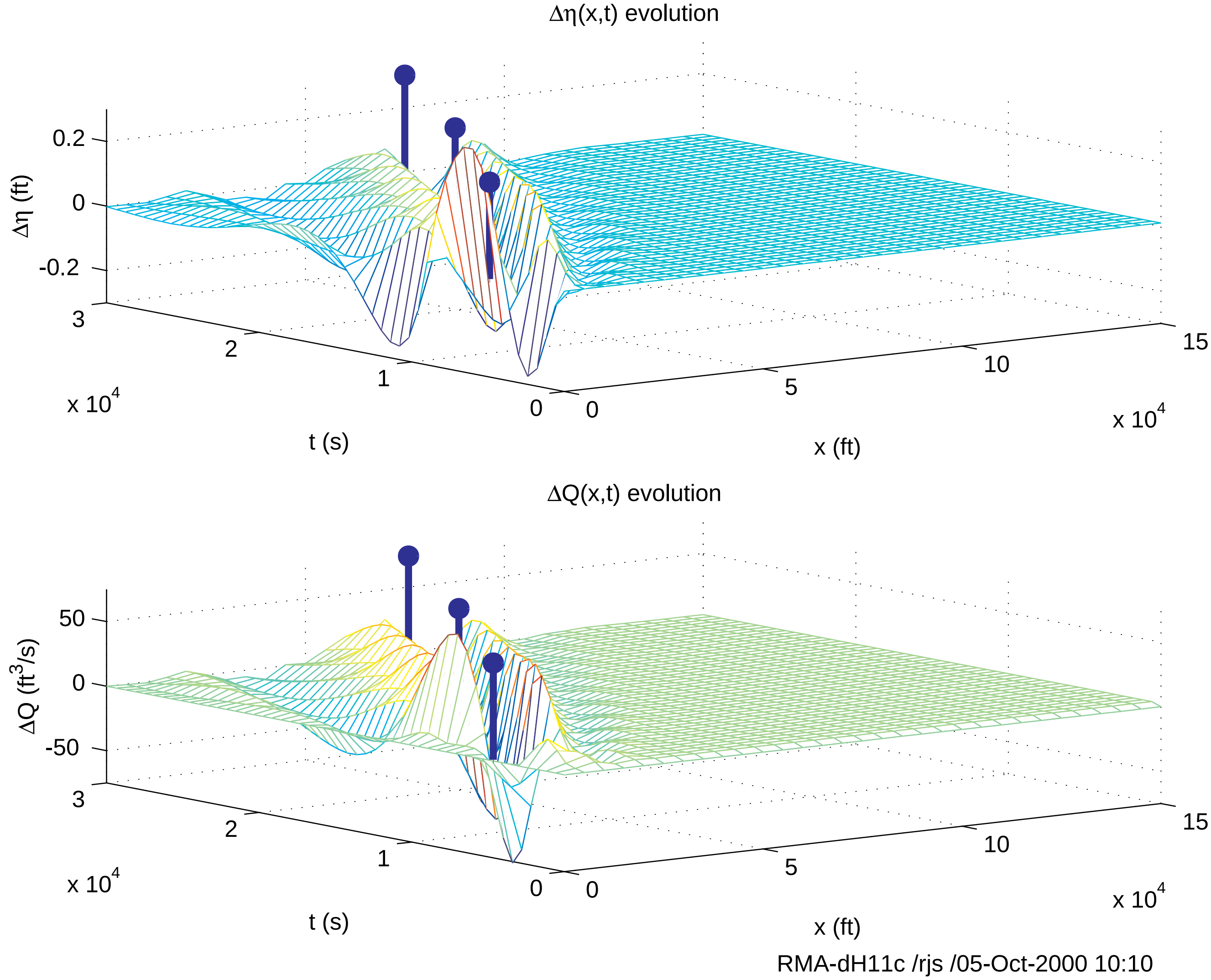

Figure 14.15: Error evolution in H11c RMA prediction.